Operating pressure dependence of the pressurized oxy-fuel combustion power cycle

Citation: Hong, Jongsup, Randall Field, Marco Gazzino, and Ahmed F. Ghoniem. "Operating pressure dependence of the pressurized oxy-fuel combustion power cycle." Energy 35:12 (December 2010), pp. 5391-5399.

As Published: http://dx.doi.org/10.1016/j.energy.2010.07.016

Publisher: Elsevier

Persistent URL: http://hdl.handle.net/1721.1/105420

Version: Author's final manuscript: final author's manuscript post peer review, without publisher's formatting or copy editing

OPERATING PRESSURE DEPENDENCE OF THE PRESSURIZED OXY-FUEL COMBUSTION POWER CYCLE

Jongsup Hong [a], Randall Field [b], Marco Gazzino [c], Ahmed F. Ghoniem [a,*]

[a] *Department of Mechanical Engineering, Massachusetts Institute of Technology, 77 Massachusetts Avenue, Cambridge, MA 02139-4307, USA*

[b] *MIT Energy Initiative, Massachusetts Institute of Technology, 77 Massachusetts Avenue, Cambridge, MA 02139-4307, USA*

[c] *ENEL Ingegneria e Innovazione S.p.A., 56122, Pisa, Via Andrea Pisano 120, ITALY*

Key Words: oxy-fuel combustion; power cycle analysis; CO_2 capture and sequestration

ABSTRACT

Oxy-fuel combustion technology is an attractive option for capturing carbon dioxide (CO_2) in power generation systems utilizing hydrocarbon fuels. However, conventional atmospheric oxy-fuel combustion systems require substantial parasitic energy in the compression step within the air separation unit (ASU), the flue gas recirculation system and the carbon dioxide purification and compression unit (CPU). Moreover, a large amount of flue gas latent enthalpy, which has high water concentration, is wasted. Both lower the overall cycle efficiency. Pressurized oxy-fuel combustion power cycles have been investigated as alternatives. Our previous study showed the importance of operating pressure for these cycles. In this paper, as the extended work of our previous study, we perform a pressure sensitivity analysis to determine the optimal combustor operating pressure for the pressurized oxy-fuel combustion power cycle. We calculate the energy requirements of the ASU and the CPU, which vary in opposite directions as the combustor operating pressure is increased. We also determine the pressure dependence of the water-condensing thermal energy recovery and its relation to the gross power output. The paper presents a detailed study on the variation of the thermal energy recovery rate, the overall compression power demand, the gross power output and the overall net efficiency.

* Corresponding author. Tel.: +1 617 253 2295; Fax: +1 617 253 5981
E-mail address: ghoniem@mit.edu (Ahmed F. Ghoniem)

1. INTRODUCTION

Coal has been a primary energy source of electricity generation for many decades because of its availability and low costs. According to estimates by Energy Information Administration, coal accounts for over 50% of the electricity generated in the United States [1]. Coal, which is cheap and abundant, provides primary energy at a price that is the half of the cost of oil and natural gas [2]. Many researchers and policy makers agree that coal will maintain its important role in power generation in the near future [3-5].

Coal combustion emits large amounts of carbon dioxide, believed to be a significant contributor to global warming. As concerns over greenhouse gas emissions grow, scientists and investigators have endeavored to find a way to decrease carbon dioxide emissions from coal-fired power plants. Carbon dioxide capture and sequestration (CCS) technologies should play a critical role in this regard, enabling coal to continue to satisfy an increasing fraction of worldwide energy needs [6]. Oxy-fuel combustion system is one of the promising CCS options.

Current research progress suggests that pressurized oxy-coal combustion power cycles utilize the higher heating value of a fuel, produce more gross power and have higher net efficiencies than conventional atmospheric oxy-coal combustion power systems. Based on a patented pressurized oxy-coal combustion process and technology, ISOTHERM®, ENEL has conducted a number of experimental studies that show the advantages arising from pressurized conditions [7-9]. It is shown that the pressurized systems have the increased heat transfer rates in the Heat Recovery Steam Generator (HRSG), possibilities to burn cheap coals and the reduced size of components. These benefits are demonstrated by using a refractory lined combustor at 4 bars on a 5 MW_{th} system [10-14]. CANMET and ThermoEnergy have examined the pressurized oxy-coal combustion systems as well, in terms of technical and economic studies. Their studies show that the high-pressure oxy-combustion systems have benefits of low efficiency penalties and reduction in capital costs, compared to the conventional atmospheric oxy-fuel power cycles [15-21].

In our previous study, an oxy-fuel combustion power cycle utilizing a pressurized coal combustor [22] was analyzed, starting with the process design proposed by Gazzino et al. [13] for the integration of pressurized oxy-combustion with Rankine cycle. In the pressurized oxy-fuel system, oxygen is pre-compressed in the ASU where

the mass flow rate is smaller than that of the flue gases into the CPU. By pre-compressing the gas stream in the ASU, the combustion flue gases are at the high pressure and the compression work duty of the CPU, which compresses the flue gases from the combustor operating pressure to 110 bars, decreases. Imposing more compression work duty on the ASU and less on the CPU, the overall system lowers the parasitic power demand. Moreover, the energy penalty associated with the oxygen compression work required to feed oxygen into the pressurized combustor is partially offset by removing the pre-heater from the oxygen compression line, hence avoiding the thermal energy penalty related to oxygen pre-heating. In addition, the elevated dew point and higher available latent enthalpy in the flue gases lead to higher thermal energy recovery from the flue gases. The available latent enthalpy is defined as the recoverable amount of the latent enthalpy of the water in the flue gases (hot stream) based on the inlet and outlet temperatures of the feedwater (cold stream) across the heat exchanger. The increased water-condensing thermal energy recovery enables the system to produce more gross power by eliminating the steam bleeding from the low pressure steam turbines. Compared to a conventional atmospheric oxy-fuel combustion system, the pressurized system was shown to be more efficient, taking advantage of lower overall compression work demand and higher gross power output.

Moreover, our study showed that the fan compression work has a significant impact on the overall performance. Most oxy-fuel combustion systems have implemented recirculation of the flue gases to decrease the combustion temperature to a reasonable level. Thus, a significant amount of the flue gases is re-circulated within the system, requiring a substantial amount of energy to compensate for the pressure drop across the steam generation unit and the recirculation pipe. This feature is even more important for the combustion technology patented by ITEA [7-9], which adopts two flue gas recycling lines employed to control the combustion temperature and temperature at the HRSG inlet.

Based on the finding from the previous study, we have concluded that the combustor operating pressure has a strong impact on the overall performance of the oxy-fuel system. In this paper, we perform a pressure sensitivity analysis to find the optimal combustor operating pressure. We calculate the pressure dependence of the thermal energy recovery rate, the overall parasitic power demand, the gross power output and the overall efficiency. The analysis enables us to determine which parameters are important in operating the pressurized system and to examine

how to improve the overall performance. The methodology used in the study is explained in Section 2, and the detailed results are discussed in Section 3. Section 4 includes conclusions.

2. METHODOLOGY

A 300 MW_e coal-fired power plant, which is based on the fixed coal flow rate of 30 kg/s corresponding to 874.6 MW_{th} (HHV) or 839.1 MW_{th} (LHV), is used as the base case for the pressure sensitivity analysis. In the previous study, we proposed the pressurized oxy-fuel combustion power cycle and discussed its characteristics. The cycle has been modified to include the best available technologies; all important design variables are shown in Section 2.1. The combustor operating pressure was controlled by changing the oxygen delivery pressure to the combustor from 1.238 bars to 30 bars. The proposed approach will be explained and discussed in the following sections.

Two commercial simulation packages, Thermoflex® and Aspen Plus®, were used to conduct the study. An integration method between these two simulation tools is mentioned in the previous paper [22]. Aspen Properties® provides thermodynamic and transport properties used to estimate the pressure drop through the flue gas recirculation path, as explained in Section 2.2.[1]

2.1. Base Case and Design Variables

The pressure sensitivity analysis was performed using the base case we developed in our previous study [13, 22], which is revised to adopt the best available technologies especially in a steam cycle and the CPU. The base case plant consists of five primary units, the ASU, a pressurized coal combustor, a steam generation unit, a power island and the CPU. Each unit represents commercially available technologies or processes at an advanced development stage. Figure 1 shows the overall process diagram for the base case cycle for the pressurized oxy-fuel combustion system. As shown in Figure 1, after being compressed by the first feedwater pump, the condensate

[1] Thermoflex®, Aspen Plus® and Aspen Properties® are registered trademarks of Thermoflow LTD and Aspen Technology, Inc., respectively.

recuperates most of the latent enthalpy in the flue gases while flowing the acid condenser. The condensate stream is heated further by cooling the combustor walls. The feedwater heating system and the HRSG receives the condensate stream, which is compressed to the supercritical state by the second feedwater pump, and generates supercritical steam. On the gas side which is represented by the red lines, the oxygen stream is mixed with the recirculated flue gases before entering the pressurized oxy-coal combustor. The combustion flue gases are cooled down by the secondary recycled flue gases. Passing through the HRSG and the acid condenser, the flue gases transfer thermal energy to the feedwater. At the end, the flue gas stream is purified and compressed by the CPU.

The proposed system has two important updates in the power island and the CPU, compared to the pressurized oxy-fuel power cycle analyzed in our previous study. Because the double reheat steam cycle is not economically beneficial, it is believed to be a non-viable option in conventional coal-fired power plants. Thus, we updated the previous base case by replacing it with a single reheat steam cycle. We also found that the turbines used in the previous study represent 20 year old technologies and have lower isentropic efficiencies. In this regard, the power island is modified to utilize the best available steam turbines based on a reference ENEL power plant that has been recently commissioned. Data provided by ENEL also accounts for the pressure drop along the steam bleeding line to the feedwater heaters. In addition, for CO_2 production or for Enhanced Oil Recovery (EOR) applications, it is common to pressurize CO_2 by a pump above 80 bars, which is beyond the CO_2 critical point [23]. The previous CPU utilizes only compressors in the CO_2 compression steps. Therefore, the updated CPU includes a pump as well as compressors to pressurize the CO_2 stream up to the delivery pressure of 110 bars. Other detailed information on the overall processes and coal analysis data can be found in our previous paper [22].

Based on the base case processes, we fixed a set of important design variables to focus on system's operating pressure dependence. Table 1 shows the design variables used in the pressure sensitivity analysis. While the gas side variables describe the characteristics of the available ASU, the combustor and the HRSG, parameters in the steam side represent the supercritical Rankine cycle.

2.2. Pressure Drop Estimation Method

As explained in the previous section, the fan compression works for the flue gas recirculation system accounts for a significant amount of the parasitic power demand in the pressurized oxy-fuel system. In this system, recirculation of 70% to 80% of the flue gases must be used in order to reduce the combustion temperature [24]. Because a considerable pressure drop occurs across the steam generation unit and the flue gas recirculation pipe, a fan is required to re-circulate the flue gases.

As expected, the pressure drop and the corresponding fan compression work depend on the combustor operating pressure. To estimate the operating pressure dependence of the fan compression work, we have to first estimate the pressure drop. From the pressure drop, ΔP, correlations [25, 26] we know that:

$$\Delta P_{HRSG} = N\chi \frac{\rho_0 V_{\max}^2}{2} f_{HRSG}, \quad \text{where } f_{HRSG} = F(\mathrm{Re}_D, \frac{S_T}{D}) \tag{1-a}$$

$$\Delta P_{pipe} = \rho f_{pipe} \frac{L}{d} \frac{V^2}{2}, \quad \text{where } f_{pipe} = F(\mathrm{Re}_d, \frac{\varepsilon}{d}) \tag{1-b}$$

Using these correlations, we are able to evaluate the pressure drop across the HRSG and the recirculation pipe, respectively. The friction factors, f, are found from the following correlations [27, 28],

$$f_{HRSG} = \chi(0.162 + \frac{0.181\times10^4}{\mathrm{Re}} + \frac{0.792\times10^8}{\mathrm{Re}^2} - \frac{0.165\times10^{13}}{\mathrm{Re}^3} + \frac{0.872\times10^{16}}{\mathrm{Re}^4}) \tag{2-a}$$

$$f_{pipe} = \{-2.0\log[\frac{(2\varepsilon/d)}{7.4} - \frac{5.02}{\mathrm{Re}_d}\log(\frac{(2\varepsilon/d)}{7.4} + \frac{13}{\mathrm{Re}_d})]\}^{-2} \tag{2-b}$$

The heat exchanger and the recirculation pipe design assumptions include,

- The correction factor: $\chi = 1.076$
- The HRSG tube diameter: $D = 50$ mm
- The HRSG tube length: $L_{tube} = 18.29$ m

- The HRSG tube transverse pitch: S_T = 100 mm
- The HRSG tube longitudinal pitch: S_L = 100 mm
- The recirculation pipe length: L (explaining the pressure drop across the valves and the curves within the recirculation path)
- The recirculation pipe diameter: d (based on the volumetric flow rate and the velocity V)
- The roughness: ε = 0.046 mm (commercial steel)
- The maximum velocity: $V_{max} \cong$ 15.5 m/s
- The density of flue gases: ρ_0 and ρ (based on the given pressure and the temperature)
- The inlet and outlet temperatures of each heat exchanger:

  $T_{H,in}$ = the inlet temperature of the flue gas stream

  $T_{H,out}$ = the outlet temperature of the flue gas stream

  $T_{C,in}$ = the inlet temperature of the feedwater stream

To calculate ΔP_{HRSG}, the following three equations [29-31] are used to evaluate the Nusselt number, $\overline{Nu}_D$; the number of transfer units, N_{tu}; and the number of tube rows, N,

$$\overline{Nu}_D = \frac{\bar{h}D}{k} = (1+\frac{2D}{3S_L})\{0.3+\frac{0.62\,\mathrm{Re}_D^{1/2}\,\mathrm{Pr}^{1/3}}{[1+(\frac{0.4}{Pr})^{2/3}]^{1/4}}[1+(\frac{\mathrm{Re}_D}{282000})^{1/2}]\} \tag{3}$$

where, $\bar{h}$ = heat transfer coefficient, k = thermal conductivity

$$N_{tu} = -(1+R^2)^{-1/2}\ln[\frac{E-1}{E+1}] \tag{4}$$

where,

$$\varepsilon = \frac{\dot{Q}}{\dot{Q}_{\max}} = \frac{\dot{m}_H c_{P,H}(T_{H,in} - T_{H,out})}{C_{\min}(T_{H,in} - T_{C,in})} = \frac{\dot{m}_C c_{P,C}(T_{C,out} - T_{C,in})}{C_{\min}(T_{H,in} - T_{C,in})},$$

$$E = \frac{[2(F-R)/(F-1)] - (1+R)}{(1+R^2)^{1/2}}; \qquad F = \left(\frac{\varepsilon R - 1}{\varepsilon - 1}\right)^{1/n},$$

$$R = \frac{C_{\min}}{C_{\max}}; \qquad C_{\min} = \min\{\dot{m}_H c_{P,H}, \dot{m}_C c_{P,C}\}; \quad C_{\max} = \max\{\dot{m}_H c_{P,H}, \dot{m}_C c_{P,C}\}$$

$$N = \frac{N_{tu} C_{\min} S_T}{\bar{h}_c \pi D A_c} = \frac{N_{tu} C_{\min} S_T}{\bar{h}_c \pi D \dfrac{\dot{m}_H}{\rho_0 V_{\max}} \max\left\{\dfrac{S_T}{S_T - D}, \dfrac{S_T/2}{[S_L^2 + (\frac{S_T}{2})^2]^{1/2} - D}\right\}} \tag{5}$$

The number of tube rows *N* is calculated by combining (3), (4) and (5). Inserting the numbers from (2) and (5) into (1), and adding (1-a) and (1-b), we estimate the overall pressure drops across the HRSG and the recirculation pipe. The result is shown in Section 3.3.[2]

3. PRESSURE DEPENDENCE OF THE SYSTEM PERFORMANCE

The performance of the pressurized oxy-fuel power system depends on the parasitic power requirement, which includes the compression work of the ASU, the CPU and the recirculation fan, and the thermal energy recovery. Thus, the pressure dependence of these quantities must be carefully investigated.

3.1. Thermal Energy Recovery and Gross Power Output

As the combustor operating pressure rises, so does the thermal energy recovery from the flue gases that is used to generate steam. At higher pressures, the saturation temperature of the water in the flue gases rises as well. In this case, we can implement more effective thermal integration between a hot stream (flue gases) and a cold

[2] N_{tu} does not change significantly with the operating pressure because the inlet and outlet temperatures of the HRSG are fixed and the specific heat capacity of the streams remains nearly constant as the pressure increases. However, as the cross sectional area (the width) of the HRSG decreases, the number of tube rows N needed to achieve the required heat transfer surface area becomes larger.

stream (feedwater). As shown in Figure 1, the inlet temperature of the cold stream to the acid condenser, 30 °C, is determined by the steam condenser, and the maximum exit temperature of the feedwater out of the acid condenser is fixed by the deaerator operating conditions which will be discussed in the following section. Under these cold stream temperature constraints, increasing the dew point enables the latent enthalpy recovery at higher temperatures. Consequently, we can recover more latent enthalpy from the flue gases at higher temperatures with increasing the operating pressure. Figure 2 shows the dependence of the saturation temperature of the water (the blue line) and the available latent enthalpy (the red line) on the flue gas pressure. As mentioned before, the available latent enthalpy is defined as the recoverable amount of the latent enthalpy of the water in the flue gases (hot stream) based on the inlet and outlet temperatures of the feedwater (cold stream) across the acid condenser.

The available latent enthalpy increases with the operating pressure and is saturated above 10 bars, as shown in Figure 2. This is because we recover almost all HHV of the fuel as we increase the combustor operating pressure. As shown in Figure 3, the fraction of the water whose latent enthalpy is recovered through the acid condenser rises with the operating pressure. Above 10 bars, we reach nearly 100% latent enthalpy recovery rate.

Because of a large amount of water in the oxy-fuel combustion flue gases, 48% (molar) in our base case, the increase in the saturation temperature of the water enables the recovery of a significant amount of the available latent enthalpy from the flue gases. As shown in Figure 4, the total thermal energy (the blue line) recovered from the flue gases increases by nearly 6%, as the combustor operating pressure is raised from 1.238 bars to 30 bars.

The considerable increase in the thermal energy recovery lowers the regeneration heat duty from the turbines. While the conventional atmospheric oxy-fuel system cannot recover the HHV of fuel through the steam generation unit, the pressurized oxy-fuel power cycle is able to recuperate most of the HHV of the fuel because of the increased dew point as discussed above. As a result, the former needs a higher portion of the steam from steam turbines. As we recover more thermal energy from the flue gases, the regeneration heat duty and the corresponding steam bleeding from the low pressure and the intermediate pressure steam turbines decrease. Figure 4 shows the variation in the overall steam bleeding (the red line) with increase in the combustor operating pressure.

As shown in Figure 5, the gross power output increases with increasing the operating pressure, following the thermal energy recovery curve in Figure 4.

3.2. Deaerator Feedwater Inlet Temperature, Acid Condenser Pinch Point and Feedwater Mass Flow Rate

The fact that the deaerator feedwater inlet temperature should be less than the saturation temperature determines the maximum exit temperature of the feedwater out of the acid condenser. As shown in Figure 1, the condensate leaving the steam condenser flows into the acid condenser to recover the latent enthalpy from the flue gases. Next, the heated water stream enters the deaerator after recuperating more thermal energy by cooling the combustor walls. Therefore, the deaerator feedwater inlet temperature is strongly related to the amount of thermal energy recovery through the acid condenser. However, because the deaerator controls the feedwater inlet temperature so that it does not allow the feedwater to become steam before the second feedwater pump, we fix the maximum temperature we can reach at the deaerator operating pressure (10 bars in our study). Figure 6-(a) shows that the deaerator feedwater inlet temperature reaches the maximum value as the process operating pressure increases. Consequently, the deaerator operating conditions have an impact on the amount of thermal energy recovery from the flue gases through the acid condenser.

Figure 6-(b) shows another important parameter in the pressurized oxy-fuel system. As we increase the combustor operating pressure, the pinch point temperature within the acid condenser varies, as shown in Figure 6-(b). While the pinch point occurs at the dew point of the water at low pressures, it moves down to the exit temperature of the flue gas stream above 8 bars. Because the condensate temperature (inlet temperature of the cold stream to the acid condenser) is fixed by the condenser, the flue gas temperature cannot decrease any more if the pinch point occurs at the hot stream exit, which is at the condensate inlet. Therefore, the acid condenser pinch point temperature also plays an important role in the thermal energy recovery from the flue gases.

According to the change in the deaerator feedwater inlet temperature and the acid condenser pinch point, the increase in the mass flow rate of the feedwater is also limited, as shown in Figure 7.

3.3. Pressure Drop and Fan Compression Work

The pressure drop and the fan compression work play important roles in the overall performance of the pressurized oxy-fuel power system. Because the flue gas recirculation is a unique characteristic of the oxy-fuel system, it is essential to examine the related power consumption in the thermodynamic cycle analysis.

As explained in Section 2.2, the pressure drop is strongly dependent on the operating pressure. To achieve higher heat transfer coefficients, we kept the maximum velocity (V_{max}) constant within the HRSG and had denser flue gases at higher operating pressures. Given that the mass flow rate of the flue gases was held constant, maintaining the same maximum velocity was possible by reducing the width of the HRSG and, hence its cross sectional area. In addition, the diameter of the flue gas recirculation pipe was determined so as not to have a huge pipe when increasing the flue gas velocity. Because the volumetric flow rate grows as the combustor operating pressure is decreased from 10 bars to 1.238 bars, we had to linearly increase the flue gas velocity. On the other hand, above 10 bars, we kept the flue gas velocity constant because we have to keep the pipe diameter within a reasonable value as the volumetric flow rate decreases. Table 2 shows the reference velocities used in the recirculation pipe pressure drop estimation. As the pressure changes from 1.238 bars to 30 bars the diameter of the flue gas recirculation pipe is reduced as the volumetric flow rate and the reference velocity are varied.[3] Throughout the range of operating pressures, the flow in the pipe remains turbulent. Moreover, the flue gas recirculation pipe has the valves and the curves within the recirculation path. This accounts for a large amount of the pressure drop across the recirculation pipe. Figure 8-(a) shows the pressure drop across the HRSG (the blue line) and the pressure drop across the flue gas recirculation pipe (the red line). The flue gas recirculation pipe pressure drop is strongly dependent on the flue gas density, the diameter of the flue gas recirculation pipe, and the square of the flue gas velocity, see the correlation (1-b). As the operating pressure increases, the flue gas density becomes larger, and the

[3] Given the constant mass flow rate of the flue gases, the volumetric flow rate is governed by the operating pressure or density. If we hold the diameter of the flue gas recirculation pipe constant at:

a) the diameter at low P: the flue gas velocity reaches the order of 1 m/s at high pressures, and it is not appropriate to operate at this low velocity.
b) the diameter at high P: the flue gas velocity increases significantly as the operating pressure is lowered to 1.238 bars. The magnitude of this high velocity is not reasonable.

To avoid these extreme cases and operate the flue gas recirculation system at a reasonable flue gas velocity, we changed the diameter of the flue gas recirculation pipe, maintaining it within a reasonable range.

diameter of the flue gas recirculation pipe decreases as explained above. On the other hand, based on the reference velocities given in Table 2, the flue gas velocity is linearly reduced at the low pressure range and is kept constant above 10 bars. These changes lead to the flue gas recirculation pipe pressure drop shown in Figure 8-(a). As a result, a higher pressure drop is encountered as the operating pressure increases, as shown in Figure 8-(b).

Based on the pressure drop, the pressure ratios across the HRSG (the blue line) and the recirculation pipe (the red line) vary, as shown in Figure 9-(a). Pressure ratios are defined as the ratio of the inlet pressure to the outlet pressure. While the HRSG pressure ratio rises continuously like the HRSG pressure drop, the pressure ratio across the flue gas recirculation pipe decreases below 10 bars and increases above 10 bars. Because the recirculation pipe pressure drop is governed by the pipe diameter, as shown in the correlation (1-b), which is controlled by the flue gas velocity, the recirculation pipe pressure drop varies, as shown in Figure 8-(a). This variation leads to the pressure ratio across the flue gas recirculation pipe, as shown in Figure 9-(a). Combining the pressure ratios across the HRSG and the recirculation pipe, we have the overall pressure ratio across the fan, as shown in Figure 9-(b).

Because the fan compression work is a strong function of the pressure ratio, it follows the variation in the pressure ratio over the fan and has the minimum value at 10 bars, as shown in Figure 10.

3.4. ASU and CPU Compression Work

The pressurized oxy-fuel power cycle needs more compression work in the ASU than that of the atmospheric oxy-fuel system. Because the operating pressure is governed by the oxygen delivery pressure to the combustor, the ASU requires more compression work as the operating pressure increases. As shown in Figure 11, the ASU power consumption (the blue line) grows significantly by nearly 44%, as the combustor pressure is increased from 1.238 bars to 30 bars. The ASU is the biggest power consumer among the equipment implemented in the pressurized oxy-fuel system. At higher operating pressures, it is important to control the ASU power consumption to improve the overall performance of the system.

However, the larger oxygen compression work required to operate the combustor at higher pressures is partially offset by eliminating the oxygen pre-heater from the oxygen compression line. In conventional

atmospheric combustion systems, the gaseous oxygen is pre-heated by utilizing high temperature thermal energy sources such as steam or flue gases. The oxygen pre-heating steps result in thermal energy penalties and lower the overall efficiency. In contrast, the pressurized oxy-fuel power cycle reduces or eliminates the thermal duty of oxygen pre-heating while using oxygen compression.

On the other hand, because the flue gases are already at high pressures, the compression work in the CPU decreases as the operating pressure increases. The CPU compresses the CO_2-concentrated gases from the operating pressure up to 110 bars. Therefore, the increase in the operating pressure lowers the pressure ratio across the CPU, requiring less auxiliary compression work (the red line), as shown in Figure 11.

3.5. Overall Compression Work

Based on the results in Section 3.3 and 3.4, we now define the pressure dependence of the overall compression work demand in the pressurized oxy-fuel system. Figure 12 shows the variation in the overall compression work as the operating pressure increases. The total parasitic power demand follows the trend of the fan compression work shown in Figure 10. When the ASU compression work is combined with that of the CPU, their sum does not vary much with the operating pressure. As a result, the overall compression work which includes the power consumptions of the ASU, the CPU and the recirculation fan is mostly dependent on the fan compression work. We conclude that the overall parasitic power demand of the pressurized oxy-fuel system is a strong function of the flue gas recirculation power requirement. Again, the total parasitic power demand has the minimum at 10 bars as the fan compression work does.

The variation in the overall parasitic work demand points out that, in order to improve the performance of the pressurized oxy-fuel system, we should focus on the pressure drop within the flue gas recirculation path.

3.6. Net Efficiency

The pressure sensitivity analysis provides the optimal pressure, as shown in Figure 13. Based on the parasitic power requirement and the thermal energy recovery, the overall net efficiency varies as the operating pressure increases. At low pressures, gross power output, shown in Figure 5, increases and the overall compression

work, shown in Figure 12, decreases, the net efficiency grows by 3 percentage point when the combustor pressure is raised from 1.238 bar to 10 bars. On the other hand, at high pressures, the efficiency decreases slowly as the parasitic compression power dominates the overall performance. As a result, the maximum efficiency is achieved in the vicinity of the 10 bar operating pressure.

4. CONCLUSIONS

The combustor operating pressure has a critical impact on the overall performance of the pressurized oxy-fuel combustion power cycle. With increasing the operating pressure, the thermal energy recovery from the flue gases grows as we recuperate more available latent enthalpy at higher dew point. Increasing the energy recovery enables the pressurized oxy-fuel system to save some of the steam bleeding needed in the regeneration steps, and it subsequently produces more gross power. In addition, the fan compression work varies significantly with the operating pressure as the overall pressure drop across the steam generation unit and the recirculation pipe increase. While the ASU compression consumes more energy at higher pressures, the CPU requires less auxiliary energy. Consequently, the overall parasitic compression work demand is strongly dependent on the recirculation fan compression work. The maximum efficiency can be achieved in the vicinity of the 10 bar operating pressure. Given that the high pressure system raises the flue gas density and reduces equipment size, the best system from an economic point of view might be found at higher operating pressures.

The overall performance of the pressurized oxy-fuel combustion power cycle is a strong function of the thermal energy recovery from the flue gases and the energy requirement in the flue gas recirculation system. As the operating pressure increases, the variation in the net efficiency shows that the overall performance is sensitive to the change in these two parameters. Therefore, it is crucial to control the flue gas recirculation system and thermal energy recovery rate in order to improve the overall performance of the pressurized oxy-fuel combustion power cycle with increasing the operating pressure.

5. ACKNOWLEDGEMENTS

This research is financially supported by ENEL. Thermoflow and Aspen Technology provided Thermoflex®, Aspen Plus® and Aspen Properties®. Hussam Zebian's support for the evaluation of the pressure drop estimates is acknowledged.

6. REFERENCES

[1] Energy Information Administration. Annual Energy Outlook 2008, report no. DOE/EIA-0383(2008). Washington, D.C.: U.S. Department of Energy, 2008. Available from: http://www.eia.doe.gov/oiaf/aeo/pdf/0383%282008%29.pdf

[2] MIT. The future of coal, in an interdisciplinary MIT study. Cambridge, MA: MIT, 2007.

[3] Saha PC. Sustainable energy development: a challenge for Asia and the Pacific region in the 21st century. Energy Policy 2003; 31(11): 1051-1059.

[4] Zhou F, Zhou D. Study on long term energy development strategies of China. Beijing, China: China Planning Press, 1999.

[5] International Energy Agency. Roadmapping coal's future. Paris, France: OECD/IEA Coal Industry Advisory Board, 2005. Available from: http://www.iea.org/papers/2005/roadmapping.pdf

[6] Gielen D. The future role of CO_2 capture and storage: results of the IEA-ETP model, report no. EET/2003/04. Paris, France: International Energy Agency; 2003. Available from: http://www.iea.org/papers/2003/eet04.pdf

[7] Malavasi M, Rossetti E. High-efficiency combustors with reduced environmental impact and processes for power generation derivable therefrom. International patent, International publication no. WO 2005/108867, 2005.

[8] Rossetti E, Malavasi M. Method and plant for the treatment of materials, in particular waste materials and refuse. International patent, International publication no. WO 2004/094904, 2004.

[9] Malavasi M, Di Salvia G, Rossetti E. Combustion process. International patent, International publication no. WO 2009/071239, 2009.

[10] Benelli G, Malavasi M, Girardi G. Oxy-coal combustion process suitable for future and more efficient zero emission power plants. PowerGen Europe conference and exhibition. Madrid, Spain: 2007.

[11] Benelli G, Girardi G, Malavasi M, Saponaro A. ISOTHERM: a new oxy-combustion process to match the zero emission challenge in power generation. The 7th high temperature air combustion and gasification international symposium. Phuket, Thailand: 2008.

[12] Benelli G, Cumbo D, Gazzino M, Morgani E. Pressurized oxy-combustion of coal with flue gas recirculation: pilot scale demonstration. PowerGen Europe conference and exhibition. Milan, Italy: 2008.

[13] Gazzino M, Benelli G. Pressurized oxy-coal combustion Rankine-cycle for future zero emission power plants: process design and energy analysis. The 2nd international conference on energy sustainability. Jacksonville, FL, USA: 2008.

[14] Gazzino M, Riccio G, Rossi N, Benelli G. Pressurized oxy-coal combustion Rankine-cycle for future zero emission power plants: technological issues. The third international conference on energy sustainability. San Francisco, CA, USA: 2009.

[15] Zheng L, Pomalis R, Clements B. Technical feasibility study of TIPS process and comparison with other CO_2 capture power generation processes. The 32nd international technical conference on coal utilization and fuel systems. Clearwater, FL, USA: 2007.

[16] Pomalis R, Zheng L, Clements B. ThermoEnergy integrated power system economics. The 32nd international technical conference on coal utilization and fuel systems. Clearwater, FL, USA: 2007.

[17] Zheng C, Zheng L, Pomalis R, Turner R, Clements B. Conceptual design and experimental study overview: flue gas treatment and CO_2 recovery experimental system for high pressure oxygen fired coal combustion.

The 33rd international technical conference on coal utilization and fuel systems. Clearwater, FL, USA: 2008.
[18] Fassbender A. Pressurized oxy-fuel combustion for multi-pollutant capture. The 30th international technical conference on coal utilization and fuel systems. Clearwater, FL, USA: 2005.
[19] Fassbender A. Simplification of carbon capture power plants using pressurized oxyfuel. The 32nd international technical conference on coal utilization and fuel systems. Clearwater, FL, USA: 2007.
[20] Fassbender A, Tao L, Henry R. Physical properties and liquid vapor equilibrium of pressurized CO_2 rich gases from pressurized oxy-fuel combustion of coal. The 33rd international technical conference on coal utilization and fuel systems. Clearwater, FL, USA: 2008.
[21] Henry R. Modeling of pressurized oxy-fuel for recovery of latent heat and carbon capture using usibelli coal. The 32nd international technical conference on coal utilization and fuel systems. Clearwater, FL, USA: 2007.
[22] Hong J, Chaudhry G, Brisson JG, Field R, Gazzino M, Ghoniem AF. Analysis of oxy-fuel combustion power cycle utilizing a pressurized coal combustor. Energy 2009; 34(9): 1332-1340.
[23] Fradet A, Saysset S, Odru P, Broutin P, Ruer J, Bonnissel M. Technical and economic assessment of CO_2 transportation for CCS purposes. Pipeline Engineering 2007; 3rd quarter: 173-179.
[24] Buhre BJP, Elliott LK, Sheng CD, Gupta RP, Wall TF. Oxy-fuel combustion technology for coal-fired power generation. Progress in Energy and Combustion Science 2005; 31(4): 283-307.
[25] Zukauskas A, Ulinskas R. Efficiency parameters for heat transfer in tube banks. Heat Transfer Engineering 1985; 6(2): 19-25.
[26] White FM. Fluid mechanics, 5th Edition. New York: McGraw-Hill, 2003.
[27] Hewitt GF. Heat exchanger design handbook. New York/Wallingford (UK): Begell House Inc., 1998.
[28] Zigrang DJ, Sylvester ND. Explicit approximations to the solution of Colebrook's friction factor equation. AIChE 1982; 28: 514-515.
[29] Churchill SW, Bernstein M. A correlating equation for forced convection from gases and liquids to a circular cylinder in crossflow. Heat Transfer 1977; 99: 300-306.
[30] Shah RK, Mueller AC. Heat exchanger basic thermal design methods, 2nd Edition. New York: McGraw-Hill, 1985.
[31] Gnielinski V, Zukauskas A, Skrinska A. Banks of plain and finned tubes, in Hemisphere heat exchanger design handbook. Washington D.C.: Begell House, 1990.

List of Figures

Figure 1. Overall process layout for the pressurized oxy-fuel system (modified from [10])

Figure 2. Saturation temperature of the steam (the blue line) and the available latent enthalpy (the red line)

Figure 3. The fraction of the water whose latent enthalpy is recovered through the acid condenser

Figure 4. The variation in the thermal energy recovery (the blue line) and the overall steam bleeding to feedwater heaters (the red line)

Figure 5. Gross power output

Figure 6. (a) Deaerator feedwater inlet temperature and (b) acid condenser pinch point temperature

Figure 7. Deaerator feedwater inlet mass flow rate

Figure 8. (a) The HRSG pressure drop (the blue line) and the flue gas recirculation pipe pressure drop (the red line), (b) the overall pressure drop

Figure 9. (a) The pressure ratio across the HRSG (the blue line) and the pressure ratio across the flue gas recirculation pipe (the red line), (b) the pressure ratio across the fan

Figure 10. Fan compression work demand

Figure 11. Compression work demand of the ASU and the CPU

Figure 12. Overall parasitic compression work demand

Figure 13. Overall net efficiency based on HHV (the blue line) and LHV (the red line)

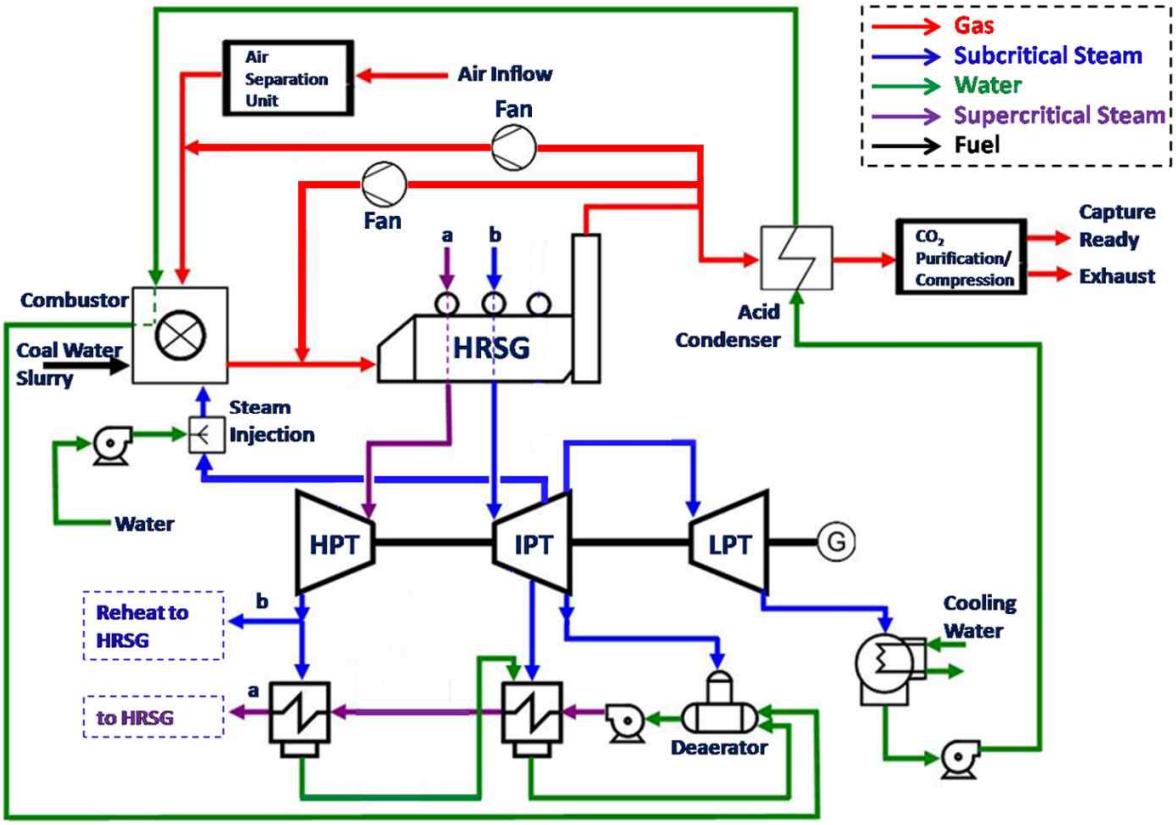

Figure 1 Overall process layout for the pressurized oxy-fuel system (modified from [10])

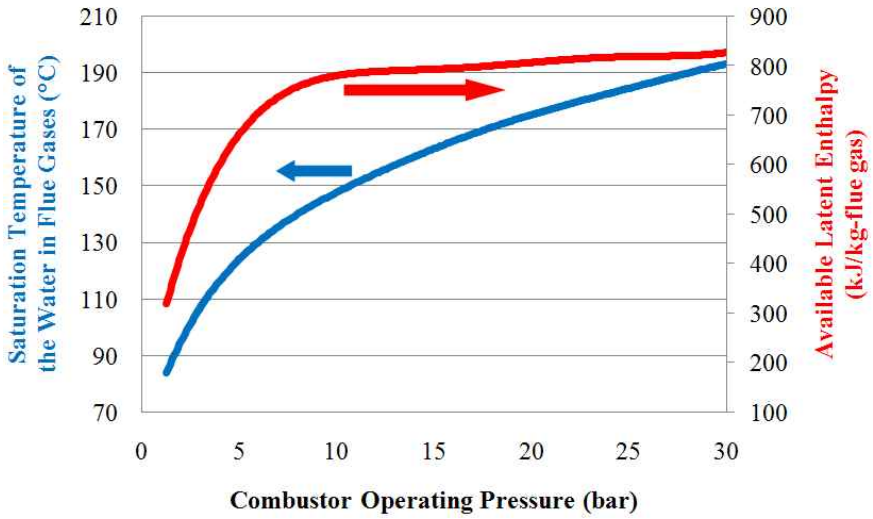

Figure 2 Saturation temperature of the steam (the blue line) and the available latent enthalpy (the red line)

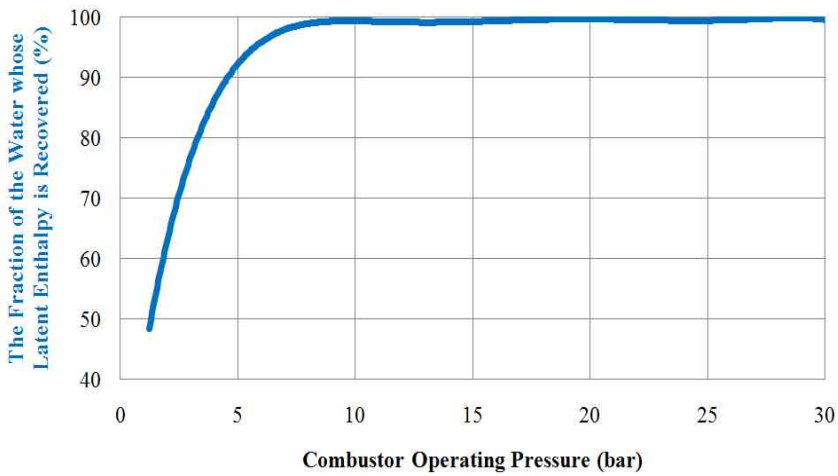

Figure 3 The fraction of the water whose latent enthalpy is recovered through the acid condenser

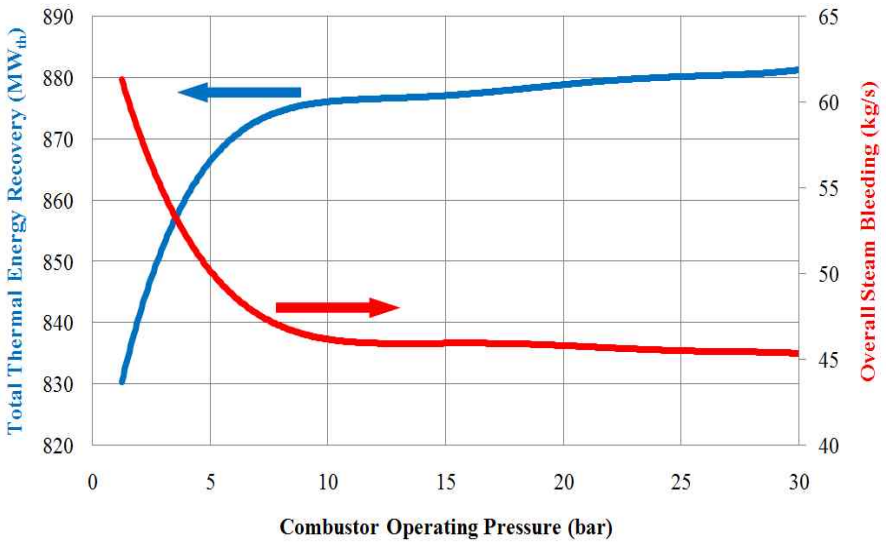

Figure 4 The variation in the thermal energy recovery (the blue line) and the overall steam bleeding to feedwater heaters (the red line)

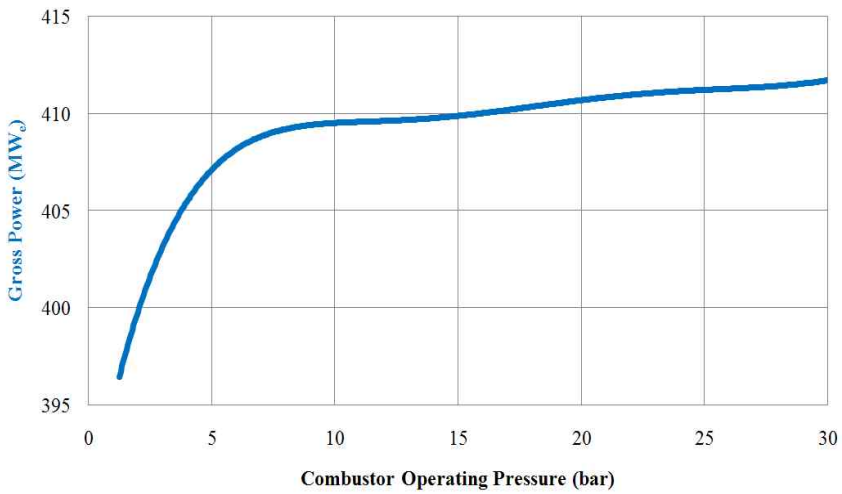

Figure 5 Gross power output

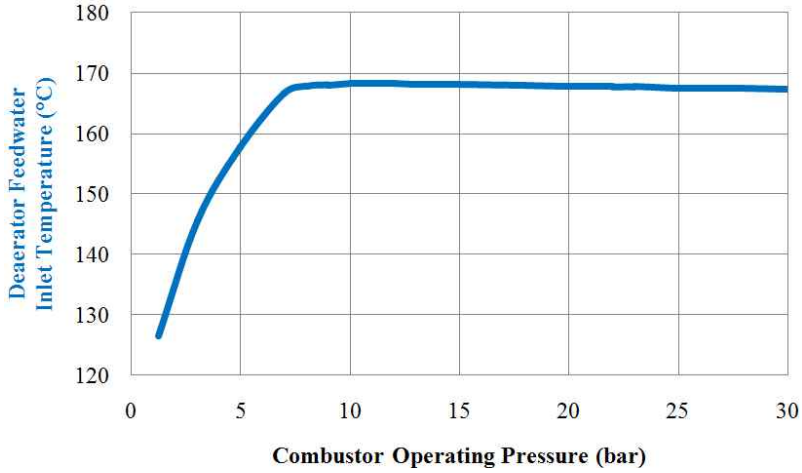

(a)

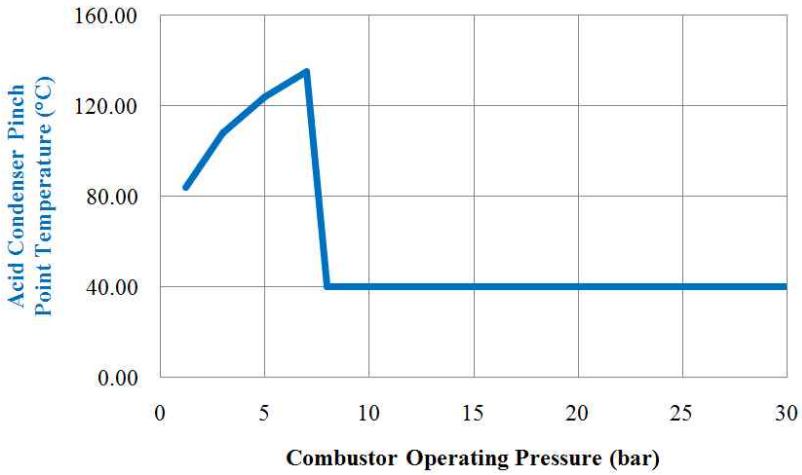

(b)

Figure 6 (a) Deaerator feedwater inlet temperature and (b) acid condenser pinch point temperature

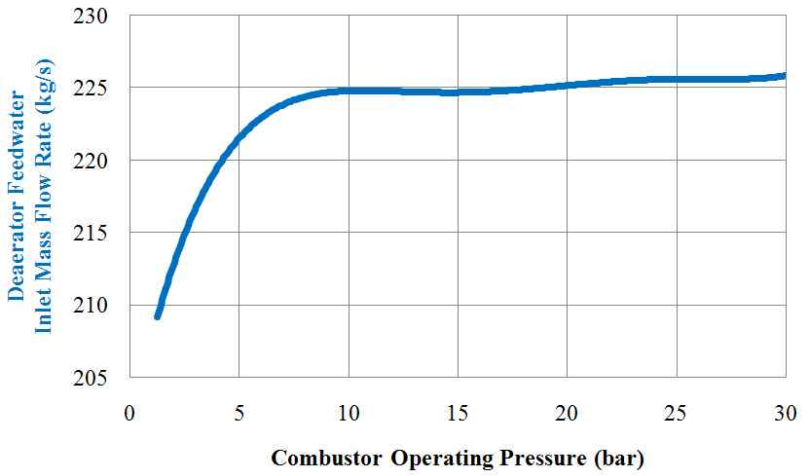

Figure 7 Deaerator feedwater inlet mass flow rate

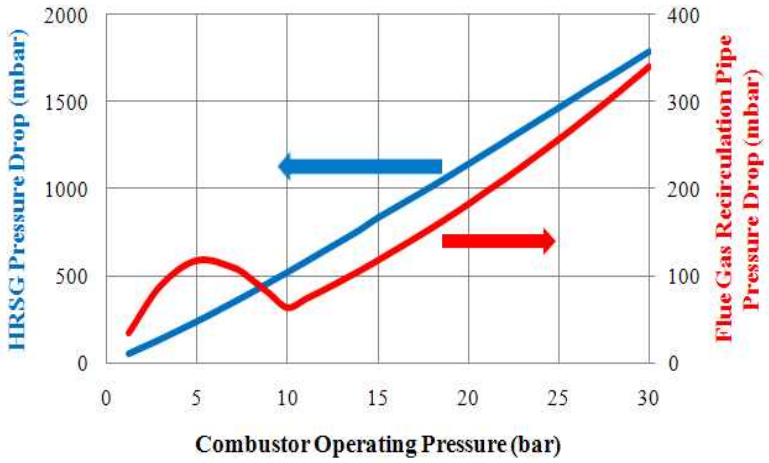

(a)

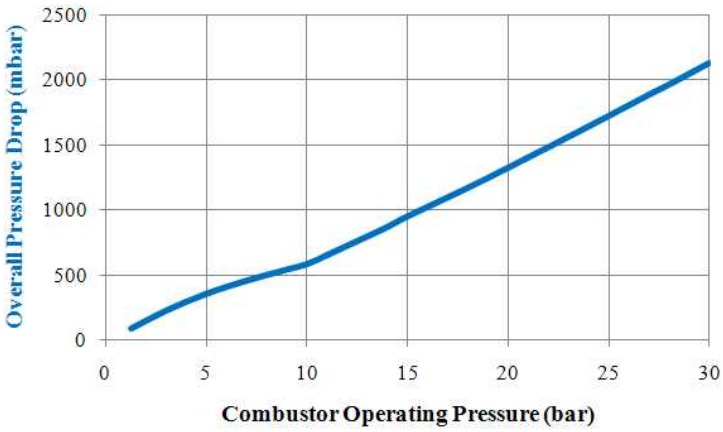

(b)

Figure 8 (a) The HRSG pressure drop (the blue line) and the flue gas recirculation pipe pressure drop (the red line), (b) the overall pressure drop

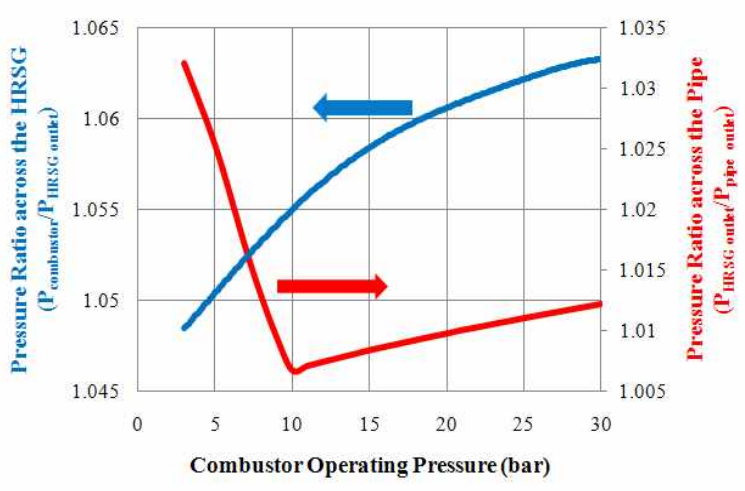

(a)

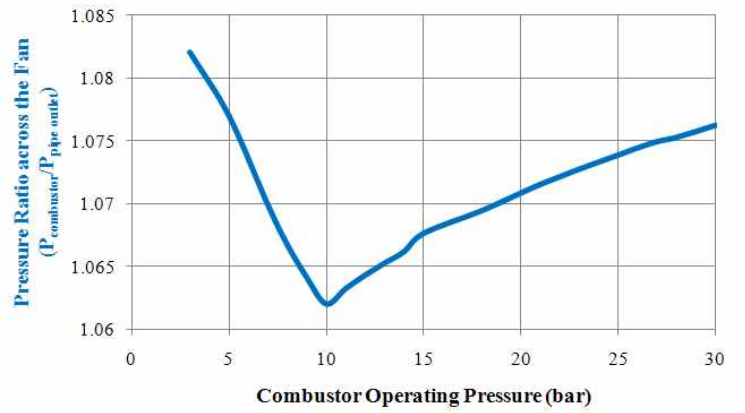

(b)

Figure 9 (a) The pressure ratio across the HRSG (the blue line) and the pressure ratio across the flue gas recirculation pipe (the red line), (b) the pressure ratio across the fan

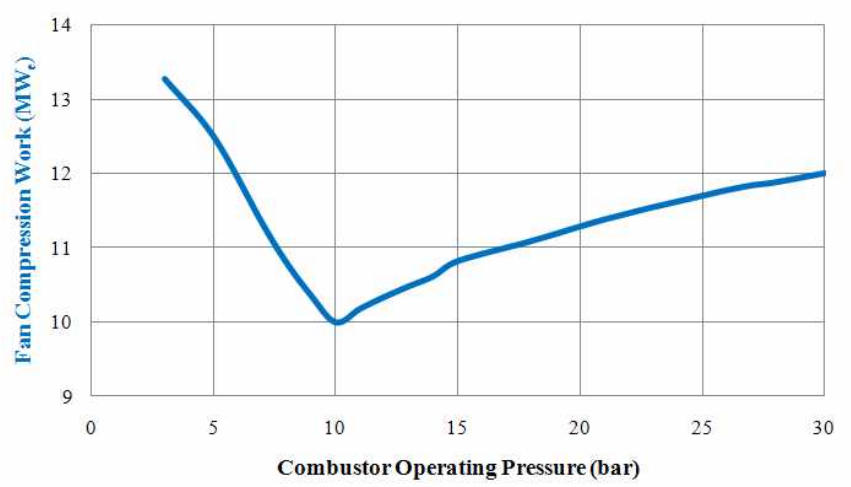

Figure 10 Fan compression work demand

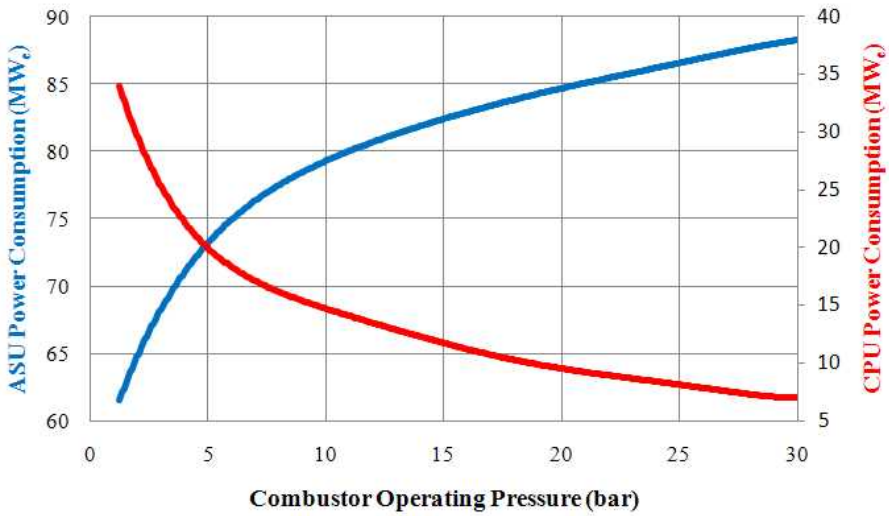

Figure 11 Compression work demand of the ASU and the CPU

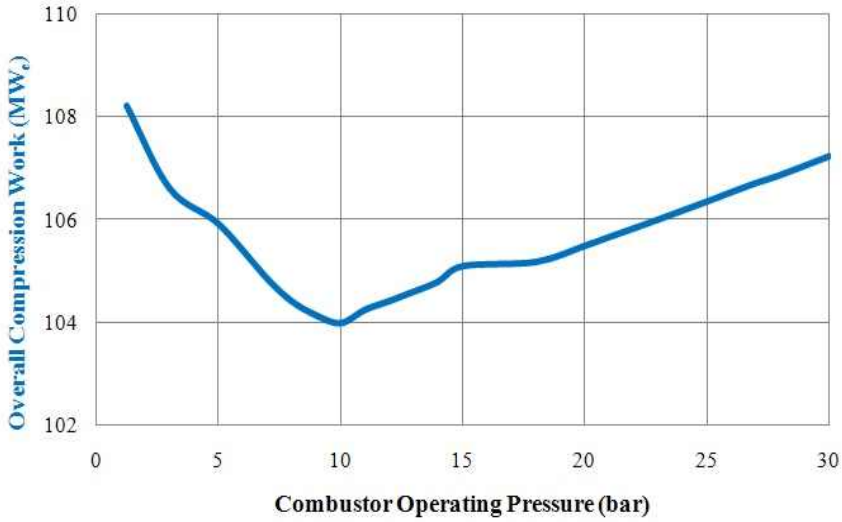

Figure 12 Overall parasitic compression work demand

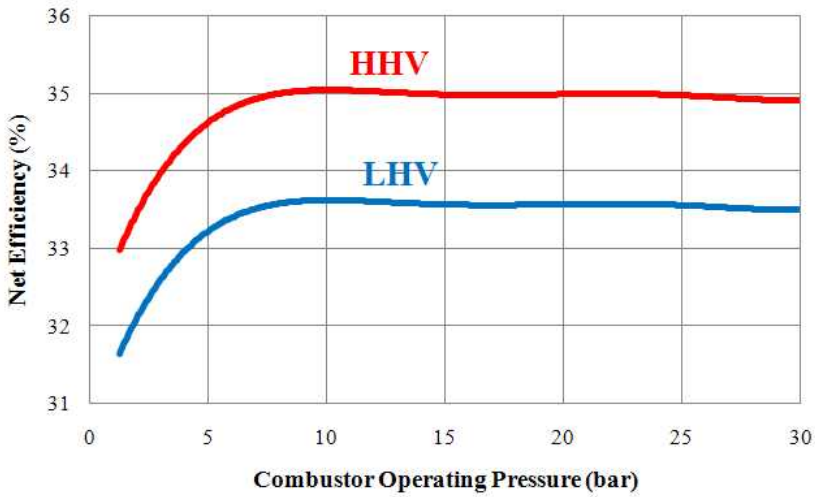

Figure 13 Overall net efficiency based on HHV (the blue line) and LHV (the red line)

List of Tables

Table 1. Design variables of the pressurized oxy-fuel system

Table 2. Reference flue gas velocities within the flue gas recirculation pipe

Table 1 Design variables of the pressurized oxy-fuel system

Design Variables	Value
Gas Side	
Oxygen Purity	95% (mol %)
Oxygen in the Flue Gas	3% (mol %)
Oxygen Delivery Temperature	200 °C
CO_2 Compression Pressure	110 bars
O_2/CO_2 Compressor Polytropic Efficiency	85%
CO_2 Pump Isentropic Efficiency	75%
Note: the combustion temperature and the inlet and outlet temperatures of the HRSG are set according to the process conditions set by ITEA and ENEL for their patented combustion technology	
Steam Side	
HPT Inlet Pressure/Temperature	250 bars/600 °C
Reheat Pressure/Temperature:	56 bars/610 °C
Turbine Isentropic Efficiency	85~96%
Deaerator Pressure	10 bars
Condenser Pressure	0.0422 bars

Table 2 Reference flue gas velocities within the flue gas recirculation pipe

	1.238 bars	10 bars
Recirculation to the combustor	25 m/s	4 m/s
Recirculation to the HRSG	30 m/s	14 m/s